Unclassified
SECURITY CLASSIFICATION OF THIS PAGE (When Data Entered)

REPORT DOCUMENTATION PAGE

READ INSTRUCTIONS BEFORE COMPLETING FORM

Field	Entry
1. REPORT NUMBER	15521.5-C
2. GOVT ACCESSION NO.	N/A AD-A103 647
3. RECIPIENT'S CATALOG NUMBER	N/A
4. TITLE (and Subtitle)	Bulk and Surface Characterization of the Silicon Electrode
5. TYPE OF REPORT & PERIOD COVERED	Reprint
6. PERFORMING ORG. REPORT NUMBER	N/A
7. AUTHOR(s)	M. J. Madou, B. H. Loo, K. W. Frese, S. Roy Morrison
8. CONTRACT OR GRANT NUMBER(s)	DAAG29-78-C-0025
9. PERFORMING ORGANIZATION NAME AND ADDRESS	SRI International, Menlo Park, CA 94025
10. PROGRAM ELEMENT, PROJECT, TASK AREA & WORK UNIT NUMBERS	N/A
11. CONTROLLING OFFICE NAME AND ADDRESS	U. S. Army Research Office, P. O. Box 12211, Research Triangle Park, NC 27709
12. REPORT DATE	1981
13. NUMBER OF PAGES	18
14. MONITORING AGENCY NAME & ADDRESS (if different from Controlling Office)	
15. SECURITY CLASS. (of this report)	Unclassified
15a. DECLASSIFICATION/DOWNGRADING SCHEDULE	

16. DISTRIBUTION STATEMENT (of this Report)

Submitted for announcement only.

17. DISTRIBUTION STATEMENT (of the abstract entered in Block 20, if different from Report)

18. SUPPLEMENTARY NOTES

19. KEY WORDS (Continue on reverse side if necessary and identify by block number)

20. ABSTRACT (Continue on reverse side if necessary and identify by block number)

Accession For
NTIS GRA&I [X]
DTIC TAB [ ]
Unannounced [ ]
Justification
By
Distribution/
Availability Codes
Dist | Avail and/or Special
A | 21

DTIC ELECTE SEP 2 1981 S D

AD A103647

DTIC FILE COPY

DD FORM 1 JAN 73 1473 EDITION OF 1 NOV 65 IS OBSOLETE

Unclassified
SECURITY CLASSIFICATION OF THIS PAGE (When Data Entered)

ARO 15521.5-C

Surface Science 108 (1981) 135–152
North-Holland Publishing Company

BULK AND SURFACE CHARACTERIZATION OF THE SILICON ELECTRODE *

M.J. MADOU, B.H. LOO, K.W. FRESE and S. Roy MORRISON
SRI International, Menlo Park, California 94025, USA

Received 8 December 1980; accepted for publication 17 February 1981

The properties of silicon as an electrode are investigated. Techniques for reproducible measurement of the doping level are described, techniques designed to avoid surface films associated with fluoride ions. A peak in the capacity/voltage curve that appears near the flatband voltage for both n- and p-type silicon is characterized in detail and shown to be associated with interface states between a surface oxide layer and the silicon. The possible chemical origin of the interface states when the electrode is in solution is discussed.

1. Introduction

The current drive for practical photoelectrochemical solar cells has renewed the interest in the silicon/electrolyte system. In this paper we present recent studies on this system where capacity measurements are used to characterize the bulk properties of silicon and to obtain information regarding interface states at the silicon/silicon oxide interface. Some of the results discussed in this paper cover a wide variety of data on the silicon/electrolyte interface, some of which were already partially known or suggested indirectly in the literature. Our contribution is thus partly new experimental data and partly new concepts that will connect and clarify otherwise disconnected observations.

In aqueous solutions the surface of the silicon anode is readily oxidized. Such an oxide layer has been shown to influence the electrode characteristics in many ways. Its presence makes the experimental determination of the flatband potential (V_{fb}) for silicon very difficult. This flatband potential is critical for the effective characterization of the energy levels of the electrode. The presence of an oxide layer has also been invoked for explaining the high Tafel slopes for hydrogen evolution on the silicon cathode [1]. It has been found also that the growth of a thin oxide increases the capacitance of the solid/liquid junction [2]. Such an increase in the form of a peak in the capacitance voltage plot will be noted below, and will

* Supported in part by the Solar Energy Research Institute and in part by the Army Research Office.

0039-6028/81/0000–0000/$02.50 © North-Holland

81 9 01 156

be attributed to the introduction of interface states as was done in ref. [2]. This additional capacitance peak in the capacitance voltage plot was elsewhere interpreted [4] as a surface state at the electrode surface. We will show here that in this case also the increased capacitance was due to an oxide film and that the interpretation in terms of interface states is preferred. The thin oxide film itself is not expected to contribute a significant series capacitance to the equivalent circuit of the electrode but only to influence the contribution of the space-charge capacitance and interface state capacitance, the latter very markedly. For these reasons it is clear that the presence of an oxide layer changes the double layer structure of the silicon/solution interface and affects the distribution of potential drops between those interfaces. Consequently, the oxide affects both the mechanism and kinetics of most electrode processes and the interpretation of measurements on the electrode in an indifferent electrolyte.

Properties of the silicon electrode that in principle do not depend on the oxide have also been reported in the literature. For example, the origin of the reverse (anodic) current for n-type silicon in the absence of a suitable stabilizing agent has been of interest. It has been suggested that the current is associated with the dissolution of silicon and that the holes participating in this dissociation process are formed in the space-charged region [3]. In more recent literature [4], some doubt has been raised about this interpretation. An alternative suggestion is that the limiting saturation current is due to thermally activated electron transfer over the barrier that exists at the semiconductor/electrolyte interface. The electrons could come, for example, from adsorbed OH^- ions. Mott–Schottky plots on "oxide free" silicon have been used [4] to determine the flatband potential for n-type silicon (in 1M KCl solution buffered to pH = 3.3 giving the value of $V_{fb} = -0.3$ V versus SCE). Another approach that has been used to estimate the flatband potential of silicon is to determine the maximum open circuit photopotential in an active solution containing ferricenium/ferrocene [5]. In another area of interest in "oxide-free" silicon, there has been reference in the literature to the presence of surface states at the "oxide-free" silicon/electrolyte interface [6]. These authors suggest such surface states may cause Fermi energy pinning in the semiconductor. From surface recombination experiments [7], it was shown, indeed, that surface states on silicon are always present. One of the surface recombination centers was shown to disappear by the addition of F^- ions.

In the present paper we attempt to reconcile the observed behavior of the silicon electrode into a single model, one wherein the oxide layer is of dominant importance. First, we will discuss the use of Mott–Schottky plots to obtain the band edge energies of the conduction and valence bands in the silicon relative to the energy levels in solution and to determine the doping level. We will show that improved results can be obtained if a stabilizing agent, rather than HF, is introduced into the solution to prevent the extensive growth of the silicon oxide layer. This permits simple and reliable Mott–Schottky plots to be obtained for both n- and p-type silicon. The interpretation of the measured flatband potential and its pH

dependence when the inevitable oxide is present will be discussed at length. Finally a considerable emphasis will be placed on the role of interface states between the silicon and the silicon dioxide in determining the electrode properties. It will be shown that recognition of the role of these interface states and the thin oxide layer on the surface of the silicon allows its very complex electrode behavior to be unraveled.

2. Results and discussion

2.1. Doping level and flatband potential measurements

The Mott–Schottky plot is a plot of C^{-2} per unit area versus the electrode potential, V, when a deep depletion region is present on the surface. From the slope of the Mott–Schottky plot, the doping level of the single crystal is obtained from the relation

$$C_{sc}^{-2} = (2/qN_D\kappa\epsilon_0)(V - V_{fb} - kT/q)\,. \qquad (1)$$

The flatband potential V_{fb} is obtained by extrapolating the C^{-2}/V relation to $C^{-2} = 0$.

The flatband potential (V_{fb}) is a measure of the energy of the valence and conduction band edges of the silicon at the silicon/electrolyte interface [8].

In order to develop a deep depletion layer on the silicon, the minority carriers must be consumed. In acidic aqueous solution, protons can capture electrons, so that minority carriers on p-type material are easily consumed. In most studies reported in the literature on n-type material HF is used in the electrolyte. In principle, holes coming to the surface form SiO_2 and the HF consumes the SiO_2. However, we have found difficulties with measurements in HF and have found other means preferable to consume holes reaching the surface.

By using an HF-free solution, we avoid the obvious problems of the attack by HF on glassware, on the reference electrode, and on the silicon masking of the electrode. More important, we are apparently able to avoid some less obvious problems such as the formation of a porous silicon film [9].

We have found for n-type silicon that linear Mott–Schottky plots can be obtained reproducibly by measuring in a solution containing 0.1M $Fe(CN)_6^{4-}$. We have reported elsewhere [10] that $Fe(CN)_6^{4-}$ is oxidized by holes in a process wherein a thin stable oxide film plays a beneficial role. Replacing HF with ferrocyanide causes the rate of oxide formation to be very low enabling us to obtain both more linear Mott–Schottky plots and more reproducible V_{fb} values. Variable voltage drops across a "thick" surface film will lead to variability in V_{fb}; consequently, V_{fb} is a sensitive measure of problems due to films.

Fig. 1, which shows a Mott–Schottky plot for an n-type monocrystalline Si sample in 0.5M KCl + 0.1M $K_4Fe(CN)_6$, illustrates the linearity of the relation over

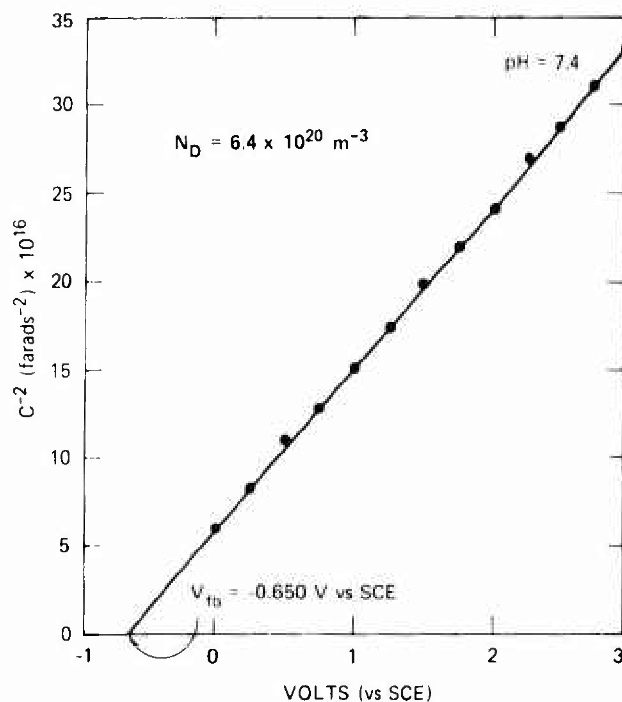

Fig. 1. Mott–Schottky plot of n-type silicon in an 0.5M KCl, 0.1M $K_4Fe(CN)_6$ aqueous solution.

a wide voltage range. The calculated donor density, indicated on the figure, is the same as that deduced from resistivity measurements. Before the measurement was made, the electrode was rinsed in 1% HF solution in the dark and then rinsed carefully with distillled water.

Reproducible Mott–Schottky measurements on p-type silicon have been much harder to obtain. The difficulty appears to be the problem of maintaining a film-free surface both before and during measurement. Because of the plentiful supply of holes, maintaining a clean surface is more difficult. Our best and most reproducible values have been obtained by etching the sample in about 20% HF and rinsing in methanol before measurement. Fig. 2 shows typical Mott–Schottky plots for p-silicon. Measurements are made in 0.1M Fe(II)EDTA. Fe(II)EDTA or $Fe(CN)_6^{4-}$ is used to consume the plentiful supply of holes during measurements on p-type material.

Fig. 3 gives the dependence of the flatband potential on pH for monocrystalline n-silicon under conditions where V_{fb} is reproducible. The pH of the ferrocyanide solution was changed by adding HCl or NH_4OH (dots and squares), the triangle represents a flatband potential obtained in 1M KCl solution, in which HCl was

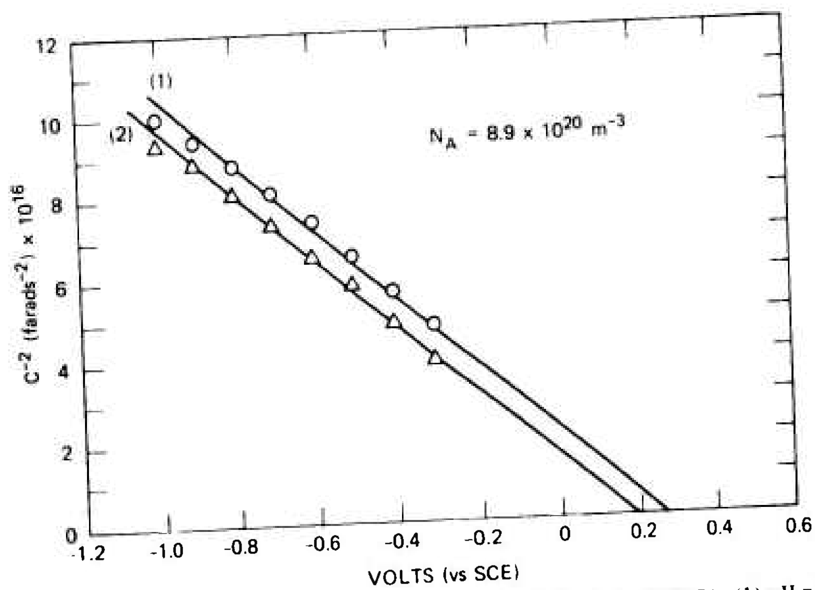

Fig. 2. Mott–Schottky plots for p-type silicon. Electrolyte: 0.1M Fe(II)EDTA; (1) pH = 2.1, (2) pH = 4.6.

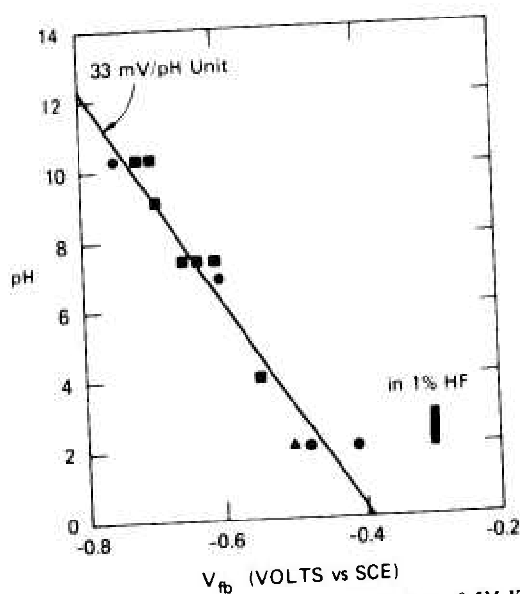

Fig. 3. Flatband potential V_{fb} versus pH for n-type silicon in an 0.5M KCl, 0.1M $K_4Fe(CN)_6$ aqueous solution.

added to adjust the pH to 2. The rectangle represents a flatband potential obtained in a solution with 0 1M $Fe(CN)_6^{4-}$, but with some HF present. The length of the rectangle reflects the uncertainty about the exact pH of this solution. The flatband potential obtained in this way is similar to the values we found in 1M KCl + 1% HF. We know from other experiments that $Fe(CN)_6^{4-}$ stabilizes Si only after formation of a thin layer of SiO_2 [10]. Hence, the difference in flatband potential in ferrocyanide solution with and without HF present presumably represents the difference between a surface covered with a very thin SiO_2 layer and an electrode with a constantly etched oxide (but possibly with some kind of thin film, or a fluoride intermediate). The slope of the graph in fig. 3 is found to be close to 30 mV/pH unit. To our knowledge, we are the first to show a plot of V_{fb} versus pH for Si. The pH dependence of the flatband potential has been shown for several other semiconductors, but usually a 60 mV/pH slope is found.

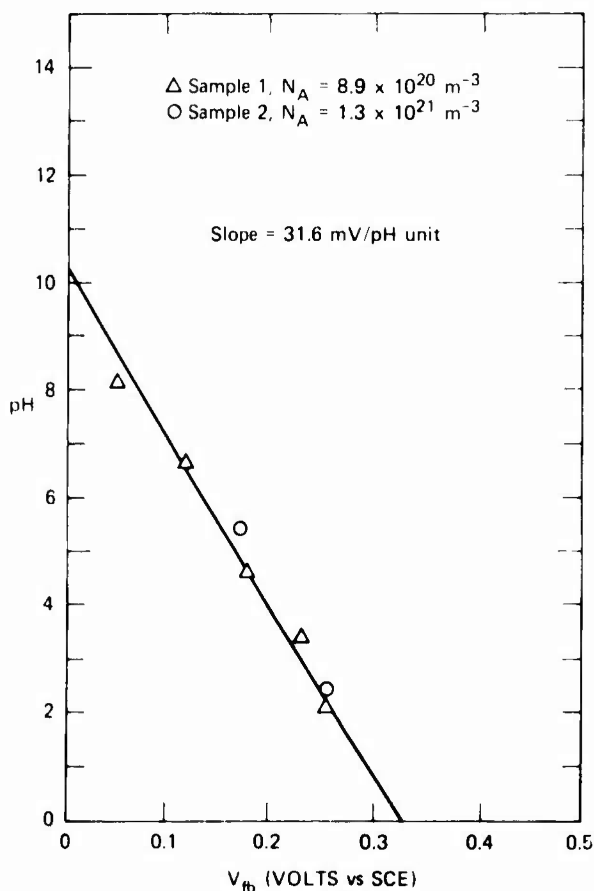

Fig. 4. Flatband potential V_{fb} versus pH for p-type silicon in the presence of Fe(II)EDTA.

Fig. 4 shows a plot of the flatband potential versus pH for p-type silicon. We note again the low sensitivity of flatband potential on pH, much lower than the 60 mV/pH unit expected from the Nernst equation. In work on the SiO_2/electrolyte interface Schenck [11] found the double layer potential change with pH was significantly less than that predicted by the Nernst equation. He also found that the double layer potential was not entirely determined by pH because it varied also with the salt concentration. Those conclusions stemmed from the observed influence of pH and salt concentration on the gate voltage. To date no solution to this problem has been offered. We also note that for any particular pH, $(V^{p}_{fb} - V^{n}_{fb}) \cong 0.7$ to 0.75 eV, compared to the expected theoretical value of $E_g - 2\mu \cong 0.7$, where V^{p}_{fb} and V^{n}_{fb} are the flatband potentials for p- and n-type silicon respectively, E_g is the energy gap (1.1 eV) and μ is the separation of the Fermi energies from the band edges, approximately the same for the two samples.

It is of interest to calculate the energy of the conduction band edge from the flatband voltage at the pH of zero charge of SiO_2 [12]. At pH = 2.2, V_{fb} is −0.47 V versus SCE. If we use the value 4.72 to convert from the SCE to the vacuum scale we obtain 4.25 eV versus vacuum for the bulk Fermi energy. In our n-type samples, $E_{CB} - E_F = 0.27$ eV, so we obtain $E_{CB} = 3.98$ eV versus vacuum. This result compares very well with the experimental value [13] of 4.01 from photoelectron emission and work function measurements and the predicted value [12] of 3.97 from electronegativity correlations. These results illustrate the accuracy of our method.

2.2. Interface state capacity

An important feature of the electrode behavior of the silicon electrode is the appearance of extra capacity over that expected from the space charge capacity as given in eq. (1). This extra capacity appears as a peak (fig. 5) when the electrode potential is near the flatband potential for either n- or p-type silicon.

There has been some discussion in the literature regarding the origin of the extra capacity. Chazalviel [4] concluded that the capacity peak is associated with surface states at the silicon/electrolyte interface and says in a footnote in the same ref. [4] that the peak does not depend on the oxide. Hurd et al. [12,14] found an increase in capacity, but did not resolve the peak. They concluded that the extra capacity is due to interface states on a film-covered surface. Memming [7] also made $C-V$ measurements on silicon in HF solutions. His measuring frequency (140 kHz) was rather high and so he did not observe a peak in the $C-V$ plot for n-type silicon. Surprisingly he observed a large peak due to surface states for p-type silicon. The height of the peak and the potential where it occurs suggests that Memming's peak must be due to another kind of surface or interface states than we are dealing with here. Turner et al. [15] also observe the capacity peak for p-silicon and suggest it is related to reduction of water in the oxide-current flow.

The frequency dependence of the capacitance peak in both cases, n- and p-Si, is readily explainable on the basis of either surface or interface states. The equivalent

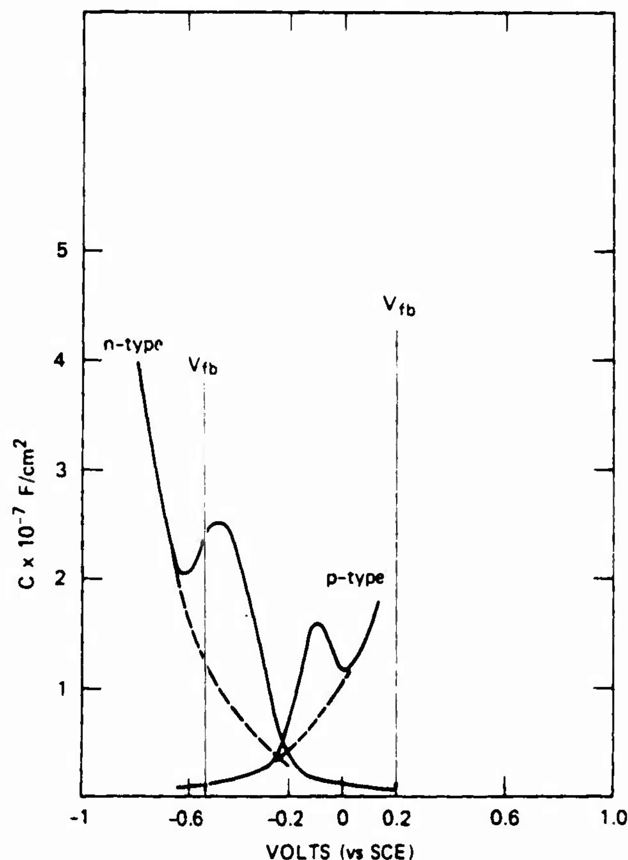

Fig. 5. Capacitance–voltage plot on n- and p-type silicon in a solution of saturated KCl buffered to pH = 4. Measuring frequency is 500 Hz. Dotted line is the expected C–V plot in the absence of interface states. Arrows indicate the flatband potentials for n- and p-type in a solution of pH = 4.

circuit for the semiconductor surface with states is indicated in fig. 6b. The space-charge capacity, which should show a linear Mott–Schottky plot, is indicated as C_{sc}. The Helmholtz capacity and the oxide capacity, which are expected to be so high as to provide negligible impedance are indicated as C_H and C_{ox} respectively. The interface state or surface capacity is C_{ss}, and is in parallel with C_{sc} [16]. The series resistance for the interface state capacity should actually be a diode, but at low ac voltage (less than kT/q) the diode can be considered equivalent to a series resistance, R_{ss}. With this circuit it is clear that at a very high frequency, such that the impedance R_{ss} is large compared to the impedance of the surface state capacity, the capacity measured will be C_{sc}. At low frequency, where the major impedance in the surface state branch of the equivalent circuit is C_{ss}, the measured capacity will

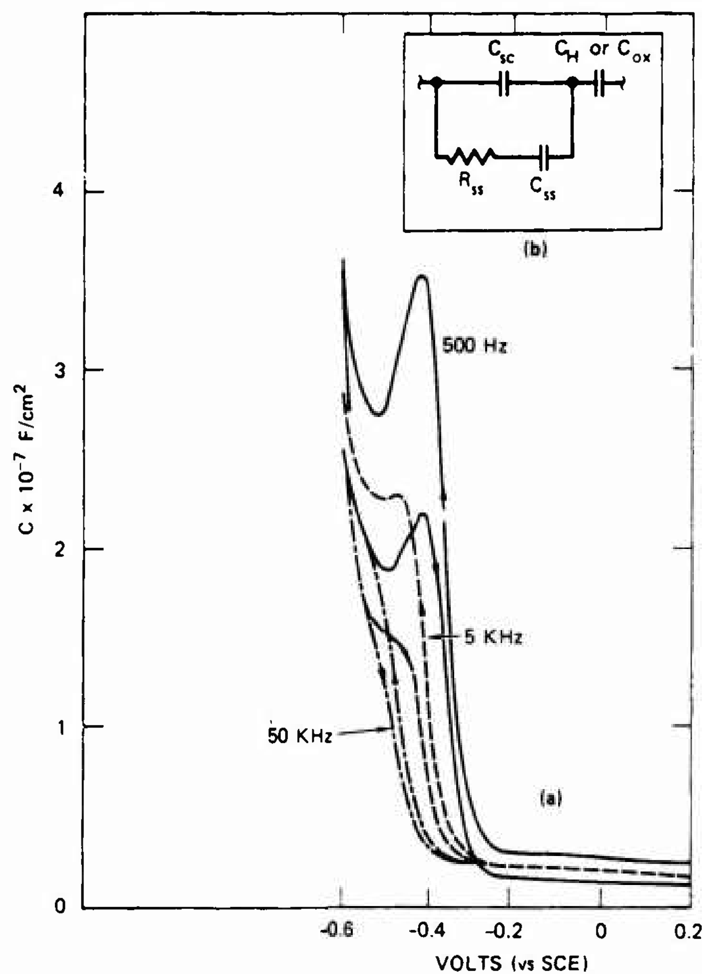

Fig. 6. (a) Capacitance–voltage plot on n-type silicon in a solution of saturated KCl buffered to pH = 4; measuring frequencies are indicated in the figure. (b) The equivalent circuit for the semiconductor surface.

be $C_{sc} + C_{ss}$. Actually the curves of fig. 5 and fig. 6a show that in the region of the peak C_{sc} is small compared to C_{ss}, and at low frequency the measured capacity must be close to C_{ss}. Thus the frequency dependence is essentially consistent with such a surface state or interface state model. In the potential range of the capacitance peak the surface charge is changing, i.e. surface or interface states are crossing the Fermi level. The further the surface states are away from the band edges, the slower the exchange of carriers in the states with the bands. When we interpret the peaks of fig. 5 in terms of interface states, it is clear that the states in the p-type

case are further away from the valence band edge than the n-type states are from the conduction band edge. This explains why the frequency dependence for p-type stretches out to lower frequencies than for n-type. Discussion of the observed hysteresis in fig. 6a will be given below.

The capacitance peak is identified as an interface capacity with the levels at the Si/SiO_2 interface rather than a surface state capacity with the levels at the solid/electrolyte interface as put forward in ref. [4]. In what follows we will give evidence for this. For example we will show that after treatment during which the oxide is expected to become thicker, namely illumination of an n-type Si anode or anodic polarization of a p-type electrode in the dark, the capacitance peak is higher and broader and remains so until the surface is rinsed with HF.

One form of evidence that the peak is indeed due to interface states is provided by measurements where a known oxide thickness is present. We find that a sample with 30 to 50 Å thickness of thermally grown oxide shows a similar peak in the capacitance–voltage curve as a sample in which the oxide is anodically grown. In

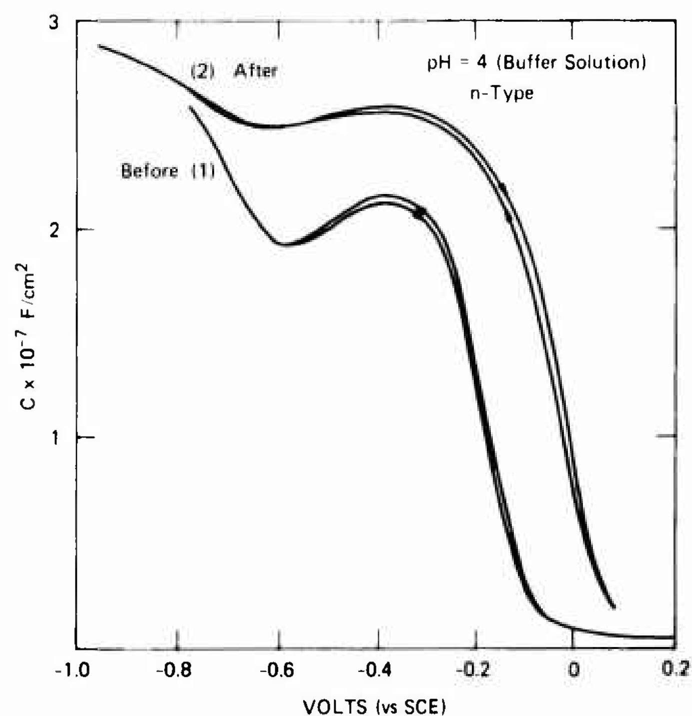

Fig. 7. (1) Capacitance–voltage plot for an a-type silicon with a thermally grown layer of SiO_2 (30–50 A). (2) Capacitance–voltage plot for an n-type silicon with a thermally grown layer of SiO_2 (30–50 A) on top of which some anodic oxide was grown. For both curves: Electrolyte is saturated solution of KCl buffered to a pH = 4. Measuring frequency is 500 Hz.

this case also the peak disappears almost completely in the presence of HF. Results on a thermally oxidized sample are shown in fig. 7 (curve 1). A comparison of fig. 7 (curve 1) with the capacitance peak in fig. 6a, where the oxide was anodically grown in our aqueous solution, shows that the main differences are the sharpness and the hysteresis for the latter. In fig. 7 (curve 2) we show the effect of anodic growth of oxide on top of the original thermal oxide. This additional anodic growth causes the peak in the capacitance voltage plot to broaden and to become higher. We suggest that the underlying reason for this is the formation of more unsaturated bonds at the Si/SiO_2 interface which contribute to the capacitance.

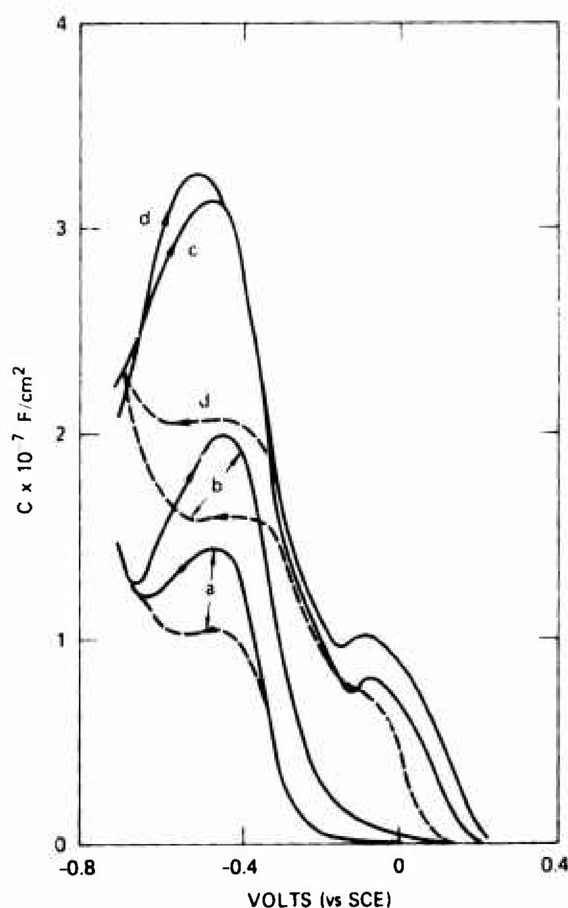

Fig. 8. Increase in C_{ss} peak due to illumination. Electrolyte 0.1M $K_4Fe(CN)_6$. (a) After HF treatment (1% HF) in the dark; (b) first sweep under illumination; (c), (d) subsequent sweeps under illumination. Only the sweep in the anodic direction is shown for (c). In all cases the sweep starts at −0.72 V versus SCE.

The increase in the excess capacity under conditions where the oxide should be developing is shown in fig. 8. Curve a in the figure is taken after an HF treatment in the dark and shows a relatively small interface state capacity peak. Then the sample is illuminated to provide holes to promote oxidation. Curve b shows the first sweep from cathodic to anodic and back (dashed) under illumination and a higher interface state capacity peak is observed that actually grows during the sweep. Curves c and d show the stable situation. As described in an earlier work [10] the action of the ferrocyanide is to prevent continued growth of the oxide, so curves c and d are reproducible. The origin of the second plateau or peak near 0 V (SCE) is due to the illumination as was also discussed in the earlier contribution. In summary, curve a shows a low surface state capacity peak following HF rinse and reimmersion in ferrocyanide solution. Some oxide presumably forms immediately for the peak is present. This is consistent with the observation [17] that about 15 Å oxide was

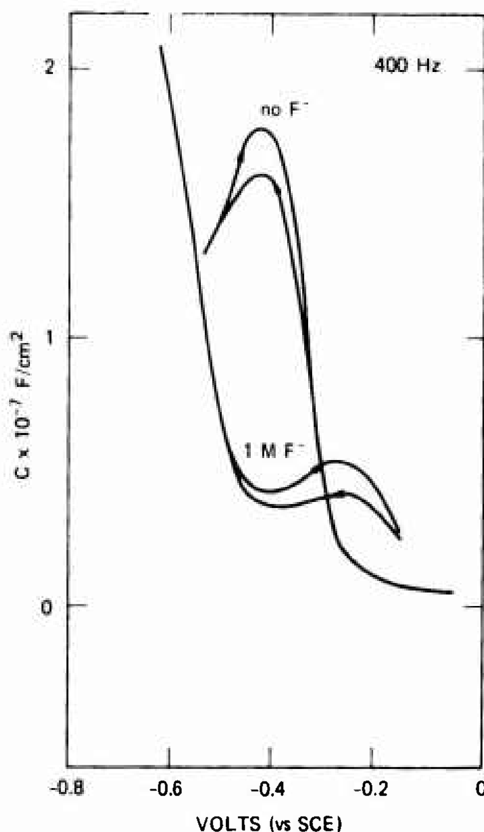

Fig. 9. Capacitance–voltage plot on n-type silicon in a solution of 1M KCl + HCl (pH ≈ 1.7) (no F^-) and the same measurement in a solution with an identical pH but with 1M F^- present. Measuring frequency is 400 Hz.

present immediately after an HF rinse. Curve b, the cycle under illumination, shows the transient condition while the oxide is growing. Curves c and d show the final condition with a thicker oxide under illumination. All measurements were made at 500 Hz.

An indication that the interface state capacity disappears with no oxide present is shown in fig. 9, where we show results for n-type silicon in HF that indicate a low interface state density. The curve with HCl present to provide a similar pH (pH = 1.7) shows a distinct interface state peak, whereas the curve with the sample in 1% HF shows a much smaller peak. Although this effect of F^- has been shown before in the literature [2,4,14] we show it again here to clarify and put in evidence two points. The first one is that in the presence of HF the peak in the capacitance voltage plot is not only lower, it is also shifted in potential of occurrence (at the same pH). This might indicate that the presence of F^- not only makes one interface state disappear but gives rise itself to another state. This was also suggested by surface recombination velocity experiments done by Memming [7]. The second point (not shown) is that at higher measuring frequency the peak in the C/V plot in the presence of HF moves also more and more towards the final capacity rise and becomes smaller and smaller. This explains why Memming measuring in HF solutions at a frequency of 140 kHz could not resolve the peak.

In order to show that oxide removal rather than F^- adsorption is the cause of the disappearance of the interface state capacity in HF, we show results in fig. 10, on n-type silicon where the fluoride ion concentration is kept constant at 1M and the pH is changed. In the curve shown, the values of pH are indicated and the significant difference of the peak height for the two cases is clear. The change in pH causes a change in flatband potential (fig. 3) and thus a shift in the position of the peak. As will be described below however, the pH has no large effect on the peak height, so the difference seen in peak height cannot be explained on that basis. Only the removal of the oxide and the resultant removal of the interface states can support the data in fig. 10.

With the above results we think that the hypothesis that the oxide is necessary for the interface states to occur is adequately supported.

The chemical origin and physical behavior of the interface states is not clear, but their response to chemical changes (e.g., pH) and physical changes (e.g. illumination) is of interest.

The influence of illumination on the capacitance peak in a condition where no additional oxide was grown is shown in fig. 11. Under illumination the peak is twice as high as that in the dark. This peak height change is reversible. It is very different from the effect described in fig. 7, where an anodic current was allowed to flow and to grow additional oxide. In that case the observed increase in the capacitance was irreversible. The reversible effect is seen on n- as well as on p-type. These results suggest a reversible photogeneration of interface states, as will be discussed further below.

The influence of the pH on the capacity peak may provide some insight into the

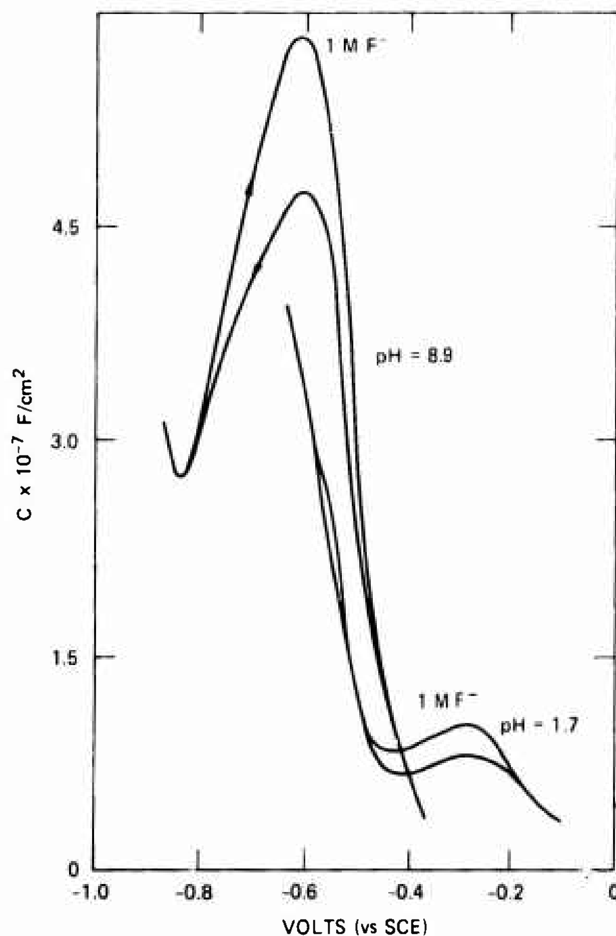

Fig. 10. Capacitance–voltage plot on n-type silicon in a solution with constant F^- concentration (1M) and varying pH.

chemical origin of the interface states, in particular their possible association with H^+ or OH^- ions. Fig. 12 shows the influence of the pH on the capacitance peaks for both a sample with about 50 Å of thermal oxide (curves in 12a) and a sample which was rinsed in a 1% HF solution before the experiment to ensure a thin oxide (curves in 12b). The pH's of the solutions, adjusted by KOH or HCl additions, are given beside the curves. The shift in the position of the peak due to a pH difference reflects the flatband potential shift as shown in fig. 3. In the case of fig. 12b, the peak appears higher in alkaline solutions but the difference is less and less pronounced the thicker the oxide gets (fig. 12a). This influence of the pH could either be associated with movement of ions (e.g., OH^-) from the solution to the inter-

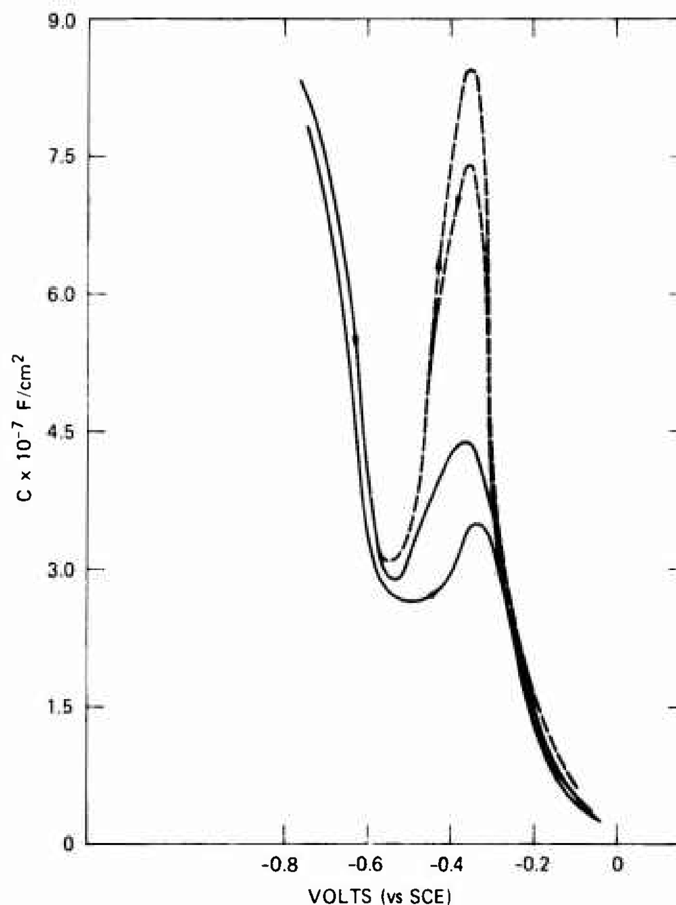

Fig. 11. Capacitance–voltage plot on n-type silicon in a saturated KCl solution buffered to pH = 10 in the dark (full line) and under illumination (dashed line). Measuring frequency is 500 Hz.

face or could be associated with a more rapid oxide growth at higher pH. Either model would be consistent with the increased effect for thinner oxides.

Another observation related to the chemical origin of the interface states, as shown quite clearly in figs. 6a, 8, 9, 10 and 11, is the dependence of the peak height on the direction in which the voltage is changing. The peak height when sweeping from anodic is lower than that sweeping from cathodic potentials. It was found for both n- and p-type that the stronger the cathodic treatment (the higher the voltage, the longer the time) the greater was the peak height during the first anodic sweep. The position of the peak is identical for the cathodic and the anodic sweep. Thus, tentatively one can conclude that the flatband potential has not

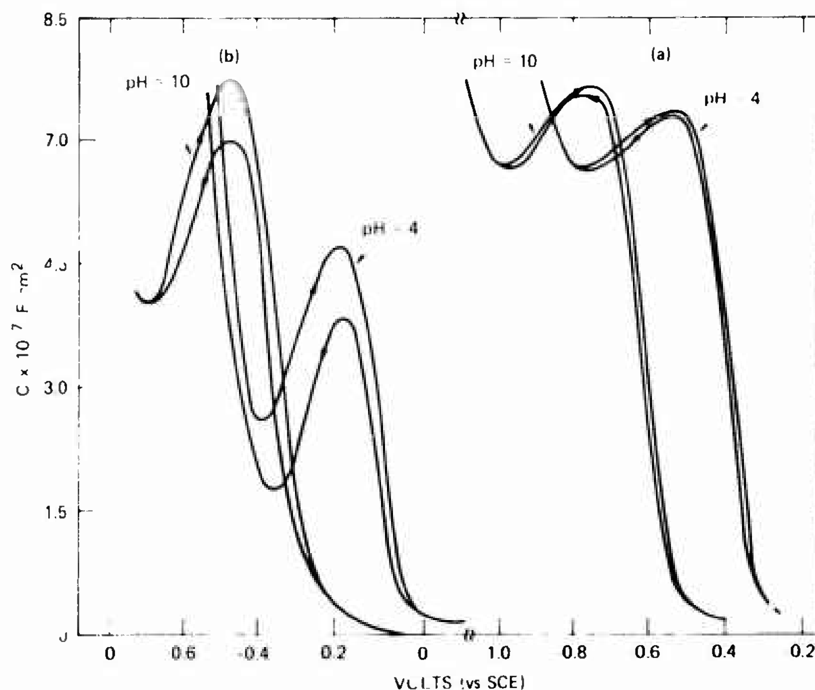

Fig. 12. (a) Capacitance–voltage plot on n-type silicon with a thermally grown layer of SiO_2 (30–50 Å) for two different pH's. (b) Capacitance–voltage plot on n-type silicon rinsed in a 1% HF solution before the measurement for two different pH's.

shifted. It seems very likely indeed that the actual density of interface states changes, depending on whether the sample has been held at a cathodic voltage or is returning from an anodic voltage.

We suggest, to explain these observations, that the interface states are associated with species (the same for n- and p-type) at the silicon/silica interface which can be forced to move to or from the interface through the oxide. For example, if the interface state were associated with Si sites, then during the anodic bias, a reaction such as

$$Si^{\cdot} + OH^- \rightarrow SiOH + e^- \qquad (2)$$

could lower the density of the Si sites, during a cathodic bias the reverse reaction could increase the density. The annihilation of the interface states in a reaction such as described above would be most rapid with very thin oxide films. Therefore the hysteresis is much more pronounced with the thin oxides and there is little hysteresis with the thick oxide in fig. 12b.

Such a model would be consistent with the photoeffect of fig. 11. Under illumination, holes would break the SiOH bonds, freeing the $Si^{\cdot}$ and increasing the effec-

tive density of surface states. With illumination only and no applied field, the OH^- or H^+ fragments would not move far, so the effective would be reversible. Other analogous reactions could explain this results.

3. Conclusions

In order to avoid subfluoride generation when holes reach the surface of silicon in an HF solution, we have found that HF should be avoided when attempting to obtain reliable doping level measurements on silicon. A stabilizing agent designed to limit the oxide growth such as ferrous ions, either in the cyano or the EDTA complex, seems to provide reliable results that do not change with time due to film formation.

An anomalously low dependence of the flatband potential on pH is not understood, but probably is due to a double layer voltage across the thin oxide that depends on pH. H^+ or OH^- ions diffusing into or through the oxide to form a space charge in the SiO_2 or at the Si/SiO_2 interface could have this effect.

A peak in the capacity/voltage curve observed with capacity measurements at low frequency is attributed to interface states. The median energy of the band of active interface levels, from the results of fig. 5, is close to the conduction band edge for n-type silicon and several tenths of a volt from the valence band edge for p-type silicon. It is shown that the detection of the interface states depends on the presence of the oxide, as could be expected. The apparent density of states depends on light intensity and on whether the sample was biassed cathodically or anodically before the measurement. We speculate that the biassing effect is associated with active ion movement through the oxide, and suggest a chemical form for the interface states depending on the presence of OH^- groups at the interface.

References

[1] E.A. Efimov and I.G. Erusalinchik, Electrochemistry of Germanium and Silicon (Sigma, Washington, 1963).
[2] R.M. Hurd and N. Hackerman, Electrochimica Acta. 9 (1964) 1633.
[3] J.B. Flynn, J. Electrochem. Soc. 105 (1958) 616.
[4] J.N. Chazalviel, Surface Sci. 88 (1979) 204.
[5] K.D. Legg, A.B. Ellis, J.M. Bolts and M.S. Wrighton, Proc. Natl. Acad. Sci. USA 74 (1977) 4116.
[6] A.J. Bard, A.B. Bocarsly, Fu-Ren F. Fan, E.G. Walton and M.W. Wrighton, J. Am. Chem. Soc. 99 (1977) 2848.
[7] R. Memming and G. Schwandt, Surface Sci. 5 (1966) 97.
[8] H. Gerischer, in: Physical Chemistry, Vol. 60A, Eds. H. Eyring, D. Henderson and W. Jost (Academic Press, New York, 1970) ch. 5.
[9] Y. Arita and Y. Sunohara, J. Electrochem. Soc. 124 (1977) 285.
[10] M.J. Madou, K.W. Frese, Jr. and S.R. Morrison, J. Phys. Chem., in press.

[11] J.F. Schenck, J. Colloid Interface Sci. 61 (1977).
[12] K.W. Frese, J. Vacuum Sci. Technol. 16 (1979) 1042.
[13] G.W. Gobeli and F.G. Allen, in: Semiconductors and Semimetals, Vol. 2, Eds. R.K. Willardson and A.C. Beer (Academic Press, New York, 1966).
[14] R.M. Hurd and P.T. Wrotenberry, Ann. NY Acad. Sci. 101 (1964) 871.
[15] J.A. Turner, J. Manassen and A.J. Nozik, J. Appl. Phys. 37 (1980) 488.
[16] S.R. Morrison, The Chemical Physics of Surfaces (Plenum, New York, 1977).
[17] R.J. Archer, J. Electrochem. Soc. 104 (1957) 619.